

## 130GeV gamma-ray line through axion conversion

Masato Yamanaka<sup>a,b,1</sup>, Kazunori Kohri<sup>b,c,2</sup>, Kunihiro Ioka<sup>b,c,3</sup>,  
and Mihoko M. Nojiri<sup>b,c,4</sup>

<sup>a</sup>*Department of Physics, Nagoya University, Nagoya 464-8602, Japan*

<sup>b</sup>*Theory Center, Institute of Particle and Nuclear Studies, KEK (High Energy Accelerator Research Organization), 1-1 Oho, Tsukuba 305-0801, Japan*

<sup>c</sup>*The Graduate University for Advanced Studies (Sokendai), 1-1 Oho, Tsukuba 305-0801, Japan*

### Abstract

We apply the axion-photon conversion mechanism to the 130 GeV  $\gamma$ -ray line observed by the Fermi satellite. Near the Galactic center, some astrophysical sources and/or particle dark matter can produce energetic axions (or axionlike particles), and the axions convert to  $\gamma$  rays in Galactic magnetic fields along their flight to the Earth. Since continuum  $\gamma$ -ray and antiproton productions are sufficiently suppressed in axion production, the scenario fits the 130 GeV  $\gamma$ -ray line without conflicting with cosmic ray measurements. We derive the axion production cross section and the decay rate of dark matter to fit the  $\gamma$ -ray excess as functions of axion parameters. In the scenario, the  $\gamma$ -ray spatial distributions depend on both the dark matter profile and the magnetic field configuration, which will be tested by future  $\gamma$ -ray observations, e.g., H.E.S.S. II, CTA, and GAMMA-400. As an illustrative example, we study realistic supersymmetric axion models, and show the favored parameters that nicely fit the  $\gamma$ -ray excess.

---

<sup>1</sup>yamanaka@eken.phys.nagoya-u.ac.jp

<sup>2</sup>kohri@post.kek.jp

<sup>3</sup>kunihito.ioka@kek.jp

<sup>4</sup>nojiri@post.kek.jp

# Contents

<b>1</b>	<b>Introduction</b>	<b>1</b>
<b>2</b>	<b>Axion-photon conversion and its application to the 130 GeV <math>\gamma</math></b>	<b>2</b>
2.1	Conversion probability . . . . .	3
2.2	Possible scenarios to fit the observed $\gamma$ -ray line . . . . .	5
2.3	Axion production . . . . .	6
2.4	Partial cross sections or decay rates fitted by observations . . . . .	7
<b>3</b>	<b>Models</b>	<b>10</b>
3.1	Axion production from decay of the long-lived dark matter . . . . .	10
3.2	Axion production from annihilation . . . . .	11
<b>4</b>	<b>Summary and discussion</b>	<b>11</b>

## 1 Introduction

Cosmological and astrophysical measurements have been supporting the existence of dark matter [1, 2]. Numerical simulations [3, 4, 5, 6] and the thermal relic scenario [7, 8] suggests that weakly interacting massive particles (WIMPs) are the most likely candidate for dark matter. Indirect detection, which searches for the annihilation and/or decay products of dark matter, is a promising way to explore its nature. Indirect detection is quite important in checking thermal relic scenarios of WIMP dark matter, because the annihilation cross section directly connects with its thermal relic abundance.

One of the aims of the Fermi telescope is to search for  $\gamma$ -ray signals from dark matter [9]. An excess of  $\gamma$  rays in the 120-140 GeV energy range was reported [10], based on public Fermi data [11] (see also [12, 13]). Detailed analysis focusing on the Galactic center concluded, with  $4.6\sigma$  C.L., that there was evidence for the  $\gamma$ -ray line [14]; other works also confirm the signals [15, 16, 17], though there is room for instrumental errors [18, 19, 20] (see also Ref. [21] and references therein). Quite recently, the Fermi-LAT Collaboration formally reported that the line signals at around  $E_\gamma = 133$  GeV have been detected at  $3.3\sigma$  ( $1.9\sigma$ ) C.L. for local (global) significance [22].

So far, no natural astrophysical models for a source of  $\gamma$ -ray lines with a narrow width,  $\Delta E/E < 0.15$ , have been proposed. Some models (e.g., see Ref. [23] and references therein) try to explain the sharp  $\gamma$ -ray line via the inverse Compton scattering of ambient photons by electrons from a neutron star in the Klein-Nishina regime; this requires the electrons in the wind to be monoenergetic with a small dispersion, less than 20%–30%. Hence, the excess of  $\gamma$  rays triggered the construction of new models of dark matter [24, 25, 26, 27, 28, 29, 30, 31, 32, 33, 34, 35, 36, 37, 38, 39, 40, 41, 42, 43, 44, 45, 46, 47, 48, 49, 50, 51, 52, 53, 54, 55, 56, 57, 58, 59, 60]<sup>5</sup>.

It is challenging to build dark matter models without conflicting with astrophysical observations. A concern is the discrepancy between the dark matter annihilation cross section that yields the correct relic density and the one that fits the observed  $\gamma$ -ray signals. Because dark matter must be electrically neutral,  $\gamma$ -ray productions from dark matter annihilations are higher-order processes. For the annihilation cross section fitting to the 130 GeV  $\gamma$  rays, therefore, tree-level

---

<sup>5</sup>See also [37] for discussions about morphology differences between the annihilation and the decay scenarios.

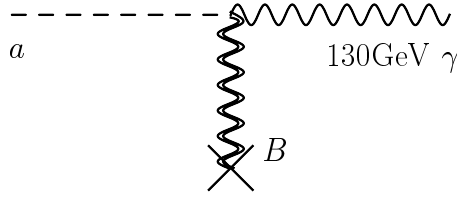


Figure 1: Axion-photon conversion in an external magnetic field  $B$ .

dark matter annihilations lead to an oversize cross section, in order to account for the measured relic density.

Another concern is the constraint on continuum  $\gamma$ -ray contributions of dark matter annihilation. Dark matters annihilate into final states (e.g.,  $W^+W^-$ ,  $Z^0Z^0$ , and so on), and their decay products produce continuum photon contributions. The ratio of the number of the continuum photons,  $N_{\text{ann}}$ , to the number of the photons responsible for the 130 GeV  $\gamma$  rays,  $N_{\gamma\gamma} + N_{\gamma Z}$ , is constrained by Fermi data. For example, in the case that the dominant annihilation products of 130 GeV dark matter are  $W^+W^-$  (or  $Z^0Z^0$ ), the constraint on the ratio is  $N_{\text{ann}}/(N_{\gamma\gamma} + N_{\gamma Z}) \lesssim 7$  [61].<sup>6</sup> The eligible dark matter candidate must therefore weakly interact with the standard model (SM) particles, except for photons. Furthermore, the hadronic contributions of annihilation (decay) products from dark matter are also constrained, by the measurement of the antiproton-to-proton ratio [63, 64] with PAMELA data [65].

In this work, we focus on the axion-photon conversion as a source of the  $\gamma$ -ray excess. We propose a scenario as follows: energetic axions are produced at the Galactic center, and the axions convert into  $\gamma$ -ray lines through the Primakoff effect in an external Galactic magnetic field [66, 67]. The axion-photon conversion and their oscillating propagation in our Galaxy have been extensively studied [68, 69, 70, 71, 72, 73]. We discuss both the conventional QCD axions and very light pseudoscalar particles that interact with electromagnetic field. The latter are called axionlike particles (ALPs). The symbol  $a$  in this work refers to both conventional axions and ALPs. (See also Refs. [74, 75, 76] for cosmological applications.)

This work is organized as follows. First, we briefly review the axion-photon conversion and evaluate its probability. Then, we evaluate the axion production cross section and the decay rate of dark matter to fit the  $\gamma$ -ray excess. In Sec. 3, as an illustrative example, we discuss supersymmetric axion models in which the 130 GeV  $\gamma$ -ray lines can be fitted. Finally, Sec. 4 is devoted to summary and discussion.

## 2 Axion-photon conversion and its application to the 130 GeV $\gamma$

We consider the scenario that energetic axions are produced at the Galactic center and that they convert into  $\gamma$  rays in an external magnetic field [66] during their flight to Earth (Fig. 1). In this scenario, the observed  $\gamma$ -ray flux  $J_\gamma$  is given by

$$J_\gamma = P_{a\gamma} \cdot J_a(E_a, \theta, \phi), \quad (1)$$

<sup>6</sup>From big bang nucleosynthesis and cosmic microwave background anisotropies, we can obtain lower limits on the flux ratio of the  $\gamma$ -ray lines to the continuum  $\gamma$ -rays,  $\gtrsim 1 \times 10^{-3}$ , commonly for  $W^+W^-$ ,  $b + \bar{b}$ , and  $e^+e^-$ 's and/or  $\gamma$ 's modes [62].

where  $P_{a\gamma}$  is the conversion probability from an axion  $a$  to a photon, and  $J_a(E_a, \theta, \phi)$  is the axion flux with energy  $E_a$ , depending on a direction  $(\theta, \phi)$ . In this section, we briefly review the conversion probability and write it in a convenient form. Next, we discuss axion production and derive the axion production cross section and the decay rate for fitting the 130 GeV  $\gamma$ -ray flux.

## 2.1 Conversion probability

The conversion process from an axion to a photon is described by the following Lagrangian:

$$\mathcal{L}_{a\rightarrow\gamma} = \frac{1}{2}(\partial^\mu a)^2 - \frac{1}{2}m_a^2 a^2 - \frac{1}{4}F_{\mu\nu}F^{\mu\nu} - \frac{1}{4}g_{a\gamma}F_{\mu\nu}\tilde{F}^{\mu\nu}a, \quad (2)$$

where  $F_{\mu\nu}$  is the electromagnetic field strength and  $\tilde{F}_{\mu\nu}$  is its dual. Here  $g_{a\gamma}$  is the effective coupling constant and  $m_a$  is the axion mass. Although  $g_{a\gamma}$  and  $m_a$  are related in QCD axion models, in this work we suppose that they are independent of each other. The current upper bound on  $g_{a\gamma}$  is obtained by the CAST experiment,  $g_{a\gamma} \lesssim 8.8 \times 10^{-11} \text{GeV}^{-1}$  for  $m_a \lesssim 0.02 \text{eV}$  [77]. The conversion probability  $P_{a\gamma}$  is given by [66, 78],

$$\begin{aligned} P_{a\gamma} &= |\langle A(t, x = L) | a(t = 0, x = 0) \rangle|^2 \\ &= \sin^2 2\Theta \sin^2\left(\frac{1}{2}qL\right), \end{aligned} \quad (3)$$

where  $L$  is the distance of the propagation and  $\Theta$  is the mixing parameter of axion and photon,

$$\sin \Theta = i\sqrt{\frac{\lambda_+}{\lambda_+ - \lambda_-}}, \quad \cos \Theta = i\sqrt{\frac{\lambda_-}{\lambda_+ - \lambda_-}}. \quad (4)$$

Here  $\lambda_\pm$  are the eigenvalues of axion-photon mixing state,

$$\lambda_\pm = \frac{1}{2} \left[ m_a^2 \pm \sqrt{m_a^4 + 4g_{a\gamma}^2 B^2 E_\gamma^2} \right]. \quad (5)$$

With the approximation  $E_a \simeq E_\gamma$ , the momentum transfer  $q$  on the conversion is calculated as follows:

$$q = \sqrt{E_\gamma^2 - \lambda_-} - \sqrt{E_\gamma^2 - \lambda_+} \simeq \frac{1}{2E_\gamma} \sqrt{m_a^4 + 4g_{a\gamma}^2 B^2 E_\gamma^2}, \quad (6)$$

in a high-energy limit  $E_\gamma \gg m_a$ . As a result, in the limit of  $E_\gamma \gg m_a$ , the conversion probability is obtained as follows:

$$\begin{aligned} P_{a\gamma} &= \sin^2 \left[ \frac{g_{a\gamma} B L}{2} \sqrt{1 + \left( \frac{m_a^2}{2g_{a\gamma} B E_\gamma} \right)^2} \right] \left[ 1 + \left( \frac{m_a^2}{2g_{a\gamma} B E_\gamma} \right)^2 \right]^{-1} \\ &= \sin^2 \left[ 2.4 \times 10 \left( \frac{L}{7.94 \text{kpc}} \right) \sqrt{\left( \frac{130 \text{GeV}}{E_\gamma} \right)^2 \left( \frac{m_a}{10^{-7} \text{eV}} \right)^4 + 3.2 \left( \frac{g_{a\gamma}}{10^{-10} \text{GeV}^{-1}} \right)^2 \left( \frac{B}{10 \mu\text{G}} \right)^2} \right] \\ &\quad \times \left[ 1 + 0.31 \left( \frac{m_a}{10^{-7} \text{eV}} \right)^4 \left( \frac{10^{-10} \text{GeV}^{-1}}{g_{a\gamma}} \right)^2 \left( \frac{10 \mu\text{G}}{B} \right)^2 \left( \frac{130 \text{GeV}}{E_\gamma} \right)^2 \right]^{-1}. \end{aligned} \quad (7)$$

In Fig. 2 we plot  $P_{a\gamma}$  as a function of  $m_a$ . We take  $g_{a\gamma} = 8.8 \times 10^{-11} \text{GeV}^{-1}$  in the top panel, which is the upper bound of  $g_{a\gamma}$ ,  $g_{a\gamma} = 1 \times 10^{-11} \text{GeV}^{-1}$  in the middle panel, and  $g_{a\gamma} = 1 \times 10^{-12} \text{GeV}^{-1}$  in the bottom panel. In each panel, the magnetic field in the Galaxy is assumed to be a uniform distribution,  $B = 10 \mu\text{G}$  (bright band) and  $B = 1 \mu\text{G}$  (dark band). The width of each

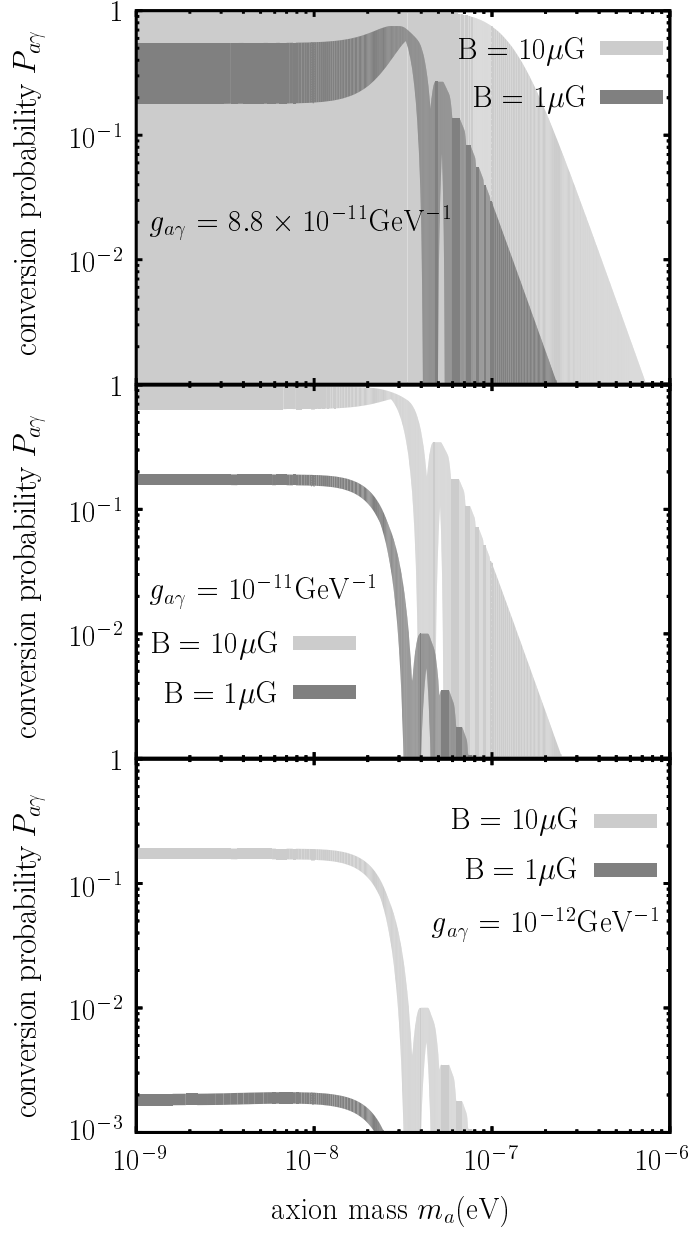


Figure 2: Conversion probability in the magnetic field,  $B = 1\mu\text{G}$ , and  $10\mu\text{G}$ . The width of each band represents ambiguities of both the energy of observed  $\gamma$ -rays and the distance from the Galactic center to the solar system. From the top to the bottom, we took the coupling constant to be  $g_{a\gamma} = 8.8 \times 10^{-11}\text{GeV}^{-1}$ ,  $1 \times 10^{-11}\text{GeV}^{-1}$ , and  $1 \times 10^{-12}\text{GeV}^{-1}$ , respectively.

band represents the ambiguities of both the energies of the  $\gamma$ -ray  $E_\gamma = 129.8 \pm 2.4_{-13}^{+7}\text{GeV}$  [14], and the distance from the Galactic center to the solar system,  $L = 7.94 \pm 0.42\text{kpc}$  [79].

In the top panel, the probability for  $B = 10\mu\text{G}$  spans a broad range. This is because the argument of sine in Eq. (7) is  $\mathcal{O}(10)$  for  $g_{a\gamma} = 8.8 \times 10^{-11}\text{GeV}^{-1}$  and  $B = 10\mu\text{G}$ . Thus,  $P_{a\gamma}$  is highly sensitive to tiny variations in  $E_\gamma$  and/or  $L$  within their ambiguities.

With the exception of the case where  $B = 10\mu\text{G}$  and  $g_{a\gamma} = 8.8 \times 10^{-11}\text{GeV}^{-1}$ , the probability is constant with  $m_a$  for the fixed  $B$  and  $g_{a\gamma}$  for lower mass regions. This is understood from Eq. (7). In Eq. (7), the term proportional to  $B^2$  in the square root in the second line is larger

than the term proportional to  $m_a^4$ , and the third line is unity. On the other hand, for larger mass regions, the terms containing  $m_a$  are dominant on both the second and third lines in Eq. (7). The third line suppresses  $P_{a\gamma}$  by a factor of  $m_a^{-4}$ , which gives oscillation damping as shown in Fig. 2.

Before closing this subsection we would like to mention magnetic field distributions in the Galaxy and magnetic field strength near the Galactic center. Because realistic magnetic field distributions remain a matter of research, we adopted a uniform distribution as a practical approximation. Another model for the distributions is the turbulent Galactic magnetic field, which is of constant magnitude and has a random direction in each small patchy domain [80]. In this model, the conversion probability per single domain is

$$P_0 \simeq \frac{g_{a\gamma}^2 \langle |B|^2 \rangle s^2 \sin^2(\pi s/l_0)}{4 (\pi s/l_0)^2}, \quad (8)$$

where  $s$  is typical size of domains and  $l_0 = 4\pi E_\gamma/m_a^2$  is the oscillation length. In the limit of  $NP_0 \ll 1$  ( $N$  is the number of domains), assuming the travelling distance  $L$  is much larger than  $s$ , the conversion probability is

$$\begin{aligned} P_{a\gamma} &= \frac{1}{3} \left[ 1 - \exp\left(-\frac{3P_0 L}{2s}\right) \right] \\ &= \frac{1}{3} \left\{ 1 - \exp\left[-3.85 \times 10^4 \left(\frac{g_{a\gamma}}{10^{-11} \text{GeV}^{-1}}\right)^2 \left(\frac{B}{10 \mu\text{G}}\right)^2 \left(\frac{E}{130 \text{GeV}}\right)^2 \left(\frac{10^{-7} \text{eV}}{m_a}\right)^4 \right. \right. \\ &\quad \left. \left. \times \left(\frac{0.01 \text{pc}}{s}\right) \left(\frac{L}{7.94 \text{kpc}}\right) \sin^2\left[3.0 \times 10^{-3} \left(\frac{s}{0.01 \text{pc}}\right) \left(\frac{130 \text{GeV}}{E_\gamma}\right) \left(\frac{m_a}{10^{-7} \text{eV}}\right)^2\right] \right] \right\}. \end{aligned} \quad (9)$$

Assuming  $s = 0.01 \text{pc}$ , for larger  $g_{a\gamma}$ , the conversion probability in the turbulent magnetic field is almost constant, and is close in value to the one in the uniform distribution. For a smaller coupling,  $g_{a\gamma} \lesssim 10^{-11}$ , assuming the same size domain, the conversion probability in the turbulent distribution is smaller than that in the uniform distribution by one or two orders.

Although the distributions are left to be considered, the large-scale magnetic field strength is steadily developing, and is indicated as  $\sim 10 \mu\text{G}$ . On the other hand, near the Galactic center, the strength can reach very high values,  $\mathcal{O}(100 \mu\text{G})$  [81]. Under such strong magnetic fields, as is given in Eq. (7), the conversion probability highly oscillates as a function of traveling distance  $L$  and the effective coupling  $g_{a\gamma}$ , and can be  $\sim 1$ . However, in such a situation, high-energy photons also have high probabilities of converting to axions. The flux ratio of axions and  $\gamma$  rays is therefore expected to be not very different with or without a very strong magnetic field near the Galactic center. Furthermore, there is no certain interpretation of the strength near the Galactic center, which possesses large uncertainties that depend on the observational data used in the analyses. Taking these facts into account, for our present purpose of showing that  $\sim 100 \text{GeV}$   $\gamma$  rays from the Galactic center are produced by the axion-photon conversion, it is acceptable way to use a uniform distribution with strength  $\sim 10 \mu\text{G}$ .

## 2.2 Possible scenarios to fit the observed $\gamma$ -ray line

Here we show scenarios explaining the 130 GeV  $\gamma$ -ray lines through the use of the axion-photon conversion. The conversion probability is an oscillating function of  $E_\gamma$  [see Eq. (7)]. In Fig. 3 we plot the conversion probability as a function of  $E_\gamma$  for some parameter sets of  $(m_a, g_{a\gamma}, B)$ . We find that observed bump shapes of  $\gamma$  rays are produced by the oscillation behavior for some

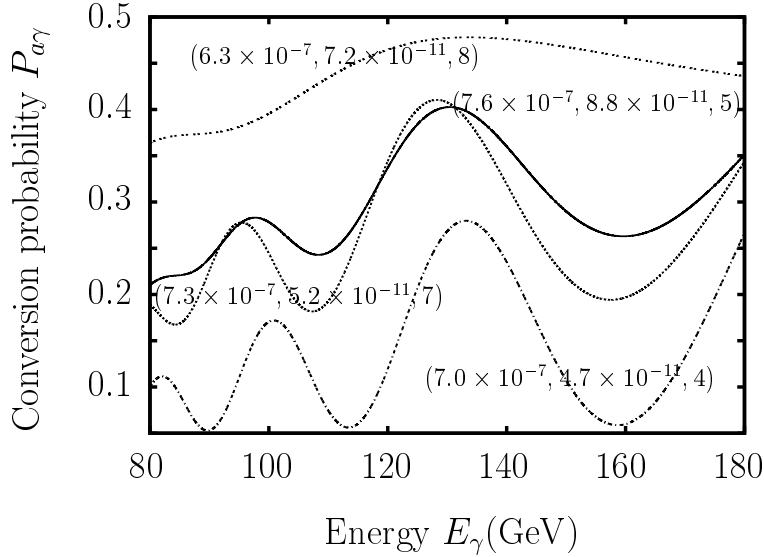


Figure 3: Conversion probabilities as a function of  $E_\gamma$ . Values on each line denote  $(m_a(\text{eV}), g_{a\gamma}(\text{GeV}^{-1}), B(\mu\text{G}))$ .

appropriate parameter sets even if the energy of the axions is not tuned to 130 GeV. Therefore we have at least two types of scenarios to fit the observational data:

- Monochromatic axions with the energy of  $\sim 130$  GeV need to be produced. Expected parameters are a large effective coupling,  $g_{a\gamma} \gtrsim 10^{-12} \text{GeV}^{-1}$ , and small axion mass  $m_a \lesssim 10^{-7} \text{eV}$  (see Fig. 2).
- It is not necessary for the axions to be monochromatic. There needs to be a fine-tuning in the sets of parameters  $(m_a, g_{a\gamma}, B)$  with a cutoff energy ( $\lesssim 200$  GeV) so that a bump shape is produced (see Fig. 3).

In this work we focus on the first scenario. An attractive candidate of the source for the monochromatic axion is a decaying or an annihilating dark matter. Thus the search for origins of the 130 GeV  $\gamma$  rays can be a bridge to the new physics that predicts dark matter. The second scenario will be discussed in a separate paper.

### 2.3 Axion production

The simplest production of energetic axions is by the decay processes of long-lived heavy particles,  $\psi$ . At the lowest order, the process is  $\psi \rightarrow a\psi'$ . Here  $\psi'$  is a stable particle, and we have assumed a  $Z_2$ -parity conservation. Under this parity, SM particles have a plus charge and  $\psi$  and  $\psi'$  have a minus charge. The  $Z_2$ -parity conservation makes  $\psi'$  ( $\psi$ ) stable (long-lived), and, hence, it is a dark matter candidate [cf., a lightest neutralino in supersymmetry (SUSY) models with R-parity conservation, a Kaluza-Klein photon in universal extra dimension models with KK-parity conservation, and so on]. We introduce a symbol  $\langle \Gamma \rangle_a$  as the partial decay width of the above process. In addition to the tree-level process, we need to draw attention to higher-order processes, which are associated with fermions in final states,  $\psi \rightarrow a\psi' f \bar{f}$ . Observations of antiprotons and continuum  $\gamma$  rays limit the production rates of these fermions. We discuss this issue later.

Another production of energetic axions is by annihilation processes of heavy neutral particles. These processes are

- $\psi\psi \rightarrow aa$
- $\psi\psi \rightarrow aZ$
- $\psi\psi \rightarrow ah$

We introduce the symbols  $\langle\sigma v\rangle_{aa}$ ,  $\langle\sigma v\rangle_{aZ}$ , and  $\langle\sigma v\rangle_{ah}$  as the cross sections of these processes. The  $Z$  boson and the Higgs boson in these processes decay into charged particles, but the production rates are limited by cosmic ray observations. We discuss this issue later.

In the next subsection, we evaluate decay rates and annihilation cross sections for the axion production to fit the observed  $\gamma$  rays.

## 2.4 Partial cross sections or decay rates fitted by observations

The most important element of this work is the proposal to fit the  $\mathcal{O}(100\text{GeV})$   $\gamma$ -ray excess from the Galactic center without conflicting with cosmic ray observations. To do this, we show that our scenario can provide the observed  $\gamma$ -ray flux through the axion-photon conversion with the appropriate axion production cross sections and decay rate. The axion production cross section and decay rate to fit the  $\gamma$ -ray excess via the axion-photon conversion are expressed by

$$\begin{aligned}\langle\sigma v\rangle_{aa(aZ,ah)} &= c_\gamma \langle\sigma v\rangle_{\gamma\gamma} / P_{a\gamma}^{\text{mean}}, \\ \langle\Gamma\rangle_a &= \langle\Gamma\rangle_\gamma / P_{a\gamma}^{\text{mean}},\end{aligned}\tag{10}$$

where  $\langle\sigma v\rangle_{\gamma\gamma}$  and  $\langle\Gamma\rangle_\gamma$  denote the  $\gamma$ -ray production cross section and decay rate that fit the observed 130 GeV  $\gamma$  rays. Here  $c_\gamma = 1$  for  $\langle\sigma v\rangle_{aa}$  and  $c_\gamma = 1/2$  for  $\langle\sigma v\rangle_{aZ(ah)}$ . The symbol  $P_{a\gamma}^{\text{mean}}$  is a mean value of the conversion probability, which is defined as follows:

$$P_{a\gamma}^{\text{mean}} \equiv \frac{P_{a\gamma}^{\text{max}} + P_{a\gamma}^{\text{min}}}{2}.\tag{11}$$

Here  $P_{a\gamma}^{\text{max}}(P_{a\gamma}^{\text{min}})$  is the maximal (minimal) conversion probability within the ranges of  $E_\gamma = 129.8 \pm 2.4_{-13}^{+7}$  GeV and  $L = 7.94 \pm 0.42$  kpc [79]. In this calculation, we do not include the effects of conversions from  $\gamma$  rays to axions or reconversion processes  $a \rightarrow \gamma \rightarrow a$ . We comment about these issues in the summary and discussion.

In order to parameterize  $P_{a\gamma}$ , we introduce a parameter  $\tilde{m}_a$ , which is a border point that separates the region with regard to  $m_a$  dependence. For  $m_a \lesssim \tilde{m}_a$ ,  $P_{a\gamma}$  is almost independent of  $m_a$ , and the mean value is straightforwardly obtained from Eq. (11). We introduce a symbol  $\tilde{P}_{a\gamma}^{\text{mean}}$ , which is  $P_{a\gamma}^{\text{mean}}$  in the region  $m_a \lesssim \tilde{m}_a$ . For the oscillation damping regime,  $P_{a\gamma}^{\text{mean}}$  is parameterized as follows:

$$P_{a\gamma}^{\text{mean}} = \tilde{P}_{a\gamma}^{\text{mean}} \left(\frac{m_a}{\tilde{m}_a}\right)^{-4} \quad (\text{For } m_a \gtrsim \tilde{m}_a).\tag{12}$$

Here  $\tilde{P}_{a\gamma}^{\text{mean}}$  and  $\tilde{m}_a$  for each parameter set are listed in the fourth column of Table 1 as coefficients of  $(m_a/\tilde{m}_a)^{-4}$ , with the denominator in parentheses.

The annihilation cross section into two  $\gamma$  lines to fit the 130 GeV  $\gamma$ -ray excess is  $\langle\sigma v\rangle_{\gamma\gamma} = (1.27 \pm 0.32_{-0.28}^{+0.18}) \times 10^{-27} \text{cm}^3 \text{s}^{-1}$  with its mass  $m_{\text{DM}} = 129.8 \pm 2.4_{-13}^{+7}$  GeV in the case of the Einasto



Table 1: Mean values of conversion probabilities  $P_{a\gamma}^{\text{mean}}$ . Symbol  $\tilde{m}_a$  separates the region in regard to  $m_a$  dependence, and  $\tilde{m}_a$  for each parameter sets are given in the denominator in parentheses in fourth column.

$g_{a\gamma}$	$B$	$P_{a\gamma}^{\text{mean}}$ for $m_a \lesssim \tilde{m}_a$	$P_{a\gamma}^{\text{mean}}$ for $m_a \gtrsim \tilde{m}_a$
$8.8 \times 10^{-11}$	$1\mu\text{G}$	$3.71 \times 10^{-1}$	$3.71 \times 10^{-1}(m_a/3.70 \times 10^{-8}\text{eV})^{-4}$
	$10\mu\text{G}$	$5.00 \times 10^{-1}$	$5.00 \times 10^{-1}(m_a/1.27 \times 10^{-7}\text{eV})^{-4}$
$1 \times 10^{-11}$	$1\mu\text{G}$	$1.72 \times 10^{-1}$	$1.72 \times 10^{-1}(m_a/1.73 \times 10^{-8}\text{eV})^{-4}$
	$10\mu\text{G}$	$8.02 \times 10^{-1}$	$8.02 \times 10^{-1}(m_a/3.63 \times 10^{-8}\text{eV})^{-4}$
$1 \times 10^{-12}$	$1\mu\text{G}$	$1.88 \times 10^{-3}$	$1.88 \times 10^{-3}(m_a/1.70 \times 10^{-8}\text{eV})^{-4}$
	$10\mu\text{G}$	$1.72 \times 10^{-1}$	$1.72 \times 10^{-1}(m_a/3.63 \times 10^{-8}\text{eV})^{-4}$

profile [14]. Similarly, the best-fit lifetime for decaying into  $\gamma$  rays is  $\tau_\gamma = 1.24_{-0.44}^{+1.20} \times 10^{28}$  s [63], with a similar setup as in Ref. [14].

The axion production cross sections  $\langle\sigma v\rangle_{aa(aZ,ah)}$  and partial decay rate  $\langle\Gamma\rangle_a$  to fit the  $\gamma$ -ray excess are evaluated from  $P_{a\gamma}^{\text{mean}}$  listed in Table 1 and Eq. (10). The results are plotted in Figs. 4 and 5, respectively. In both plots we take the same reference values for  $g_{a\gamma}$  and  $B$  as the ones used in Fig. 2.<sup>7</sup> Smaller  $g_{a\gamma}$  and weaker  $B$  lead to smaller  $P_{a\gamma}$ ; hence,  $\langle\sigma v\rangle_{aa(aZ,ah)}$  and  $\langle\Gamma\rangle_a$  need to be larger. An exception is the case of the parameter  $(8.8 \times 10^{-11}, 10)$ . As is explained in Sec. 2.1, in this case,  $P_{a\gamma}$  spans a broad range, and hence its mean value is smaller than that of the parameter  $(10^{-11}, 10)$ .

In some regions in Fig. 4,  $\langle\sigma v\rangle_{aa}$  is larger than the canonical annihilation cross section, which fits the correct relic abundance in thermal relic scenarios,  $\langle\sigma v\rangle \sim 2.2 \times 10^{-26} \text{cm}^3 \text{s}^{-1}$  (e.g., see [82]). Hence, in these regions, we need nonthermal production of dark matter, e.g., through decays of another massive particle, or a large boost factor for the dark matter annihilation cross section at the Galactic center in the current Universe.

Before closing this section, we mention the constraints on the axion production cross section. In axion production, annihilation modes  $\psi\psi \rightarrow aaZ(h)$  can cause anomalous excesses of antiproton flux and continuum  $\gamma$ -ray flux from the secondary products of  $Z$  and  $h$ . From the PAMELA measurements for the antiproton-to-proton flux ratio, a constraint on the annihilation modes into  $Z$  bosons is obtained,  $\langle\sigma v\rangle_Z \lesssim 10^{-25} \text{cm}^3 \text{s}^{-1}$  in the MED propagation model [64]. The comparable constraint is obtained from the continuum  $\gamma$ -ray measurements,  $\langle\sigma v\rangle_Z \lesssim 10^{-25} \text{cm}^3 \text{s}^{-1}$  [63, 61]. Since the annihilation modes are three-body final states, in general, the cross section is smaller than that for  $\psi\psi \rightarrow aa$  by at least  $\mathcal{O}(\alpha)$ . Here,  $\alpha$  is the fine-structure constant. Thus, from the relation  $\langle\sigma v\rangle_{aaZ(h)}/\langle\sigma v\rangle_{aa} \lesssim 10^{-2}$ , we can evaluate the bound on the axion production cross section,  $\langle\sigma v\rangle_{aa} \lesssim 10^{-23} \text{cm}^3 \text{s}^{-1}$ . Note that constraints on the axion single production,  $\psi\psi \rightarrow aZ(h)$ , are more severe than those for the axion pair productions. The bound on the cross section is

<sup>7</sup>When we suppose turbulent magnetic field distributions, larger annihilation cross sections and decay rates are required to fit the  $\gamma$ -ray spectrum for smaller couplings,  $g_{a\gamma} \lesssim 10^{-11}$ . Production cross sections and decay rates that are too large, however, may conflict with cosmic ray constraints, e.g., continuum  $\gamma$ -ray contributions. Thus, if turbulent magnetic field distributions are realized, larger  $g_{a\gamma}$  would be expected, in order to explain the  $\gamma$ -ray excess.

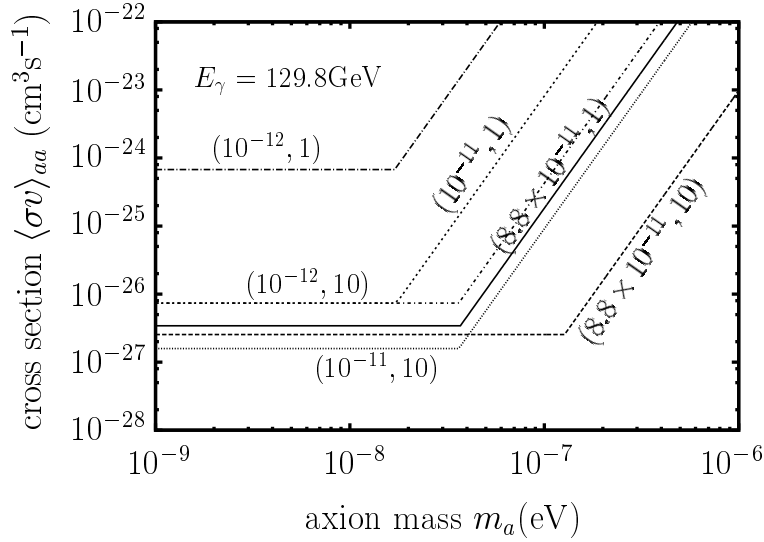


Figure 4: Annihilation cross section into axions to fit the 130GeV  $\gamma$ -ray measurements. Each label attached on the line shows the parameter set of  $g_{a\gamma}$  in unit of  $\text{GeV}^{-1}$  and B in unit of  $\mu\text{G}$ , which are the same as those used in Fig. 2.

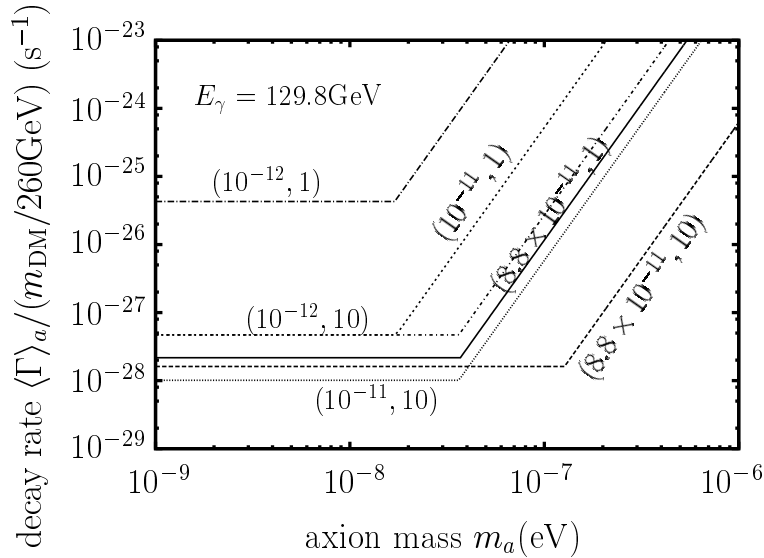


Figure 5: Same as Fig.4, but for the partial decay rate into axion.

$$\langle\sigma v\rangle_{aZ} \lesssim 10^{-25} \text{cm}^3\text{s}^{-1}.$$

In axion production from the decay process, similarly, the partial lifetimes of the modes  $\psi \rightarrow a\psi'Z$ ,  $\psi \rightarrow a\psi'h$ , and  $\psi \rightarrow a\psi'f\bar{f}$  are constrained by the measurements of the antiproton and the continuum  $\gamma$  ray,  $1/\langle\Gamma\rangle_{aZ(h)} \gtrsim 10^{27-28}\text{s}$  [64, 83]. With the same discussion as for the annihilation cross sections, the bound on the partial lifetime is  $1/\langle\Gamma\rangle_a \gtrsim 10^{25-26}\text{s}$ .

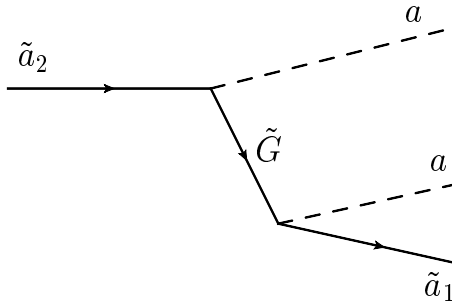


Figure 6: Decay process producing axion.

### 3 Models

In this section, as an illustrative example, we discuss two dark matter models with regard to axion productions. Our purpose here is just to show that some dark matter models surely produce monochromatic axions without producing problematic cosmic rays.

#### 3.1 Axion production from decay of the long-lived dark matter

As we have seen in Fig. 4, a preferred lifetime of the parent dark matter is around  $10^{25} - 10^{28}$  s. In Ref. [84] it is pointed out that such a long lifetime can be achieved for the process suppressed by  $1/M_{\text{GUT}}^4$ , namely, the process mediated by the GUT-scale-suppressed dimension-six operators. If such a suppressed interaction can produce axions, our scenario can be realized. On the other hand, a dimension-five GUT-scale-suppressed interaction leads to the much shorter lifetime,  $\mathcal{O}(1$  s).

One of the natural classes of models that predict dark matter is supersymmetry, and it is worth considering the possibility of realizing our scenario in the SUSY model. The lightest SUSY particle (LSP) with conserved R parity is stable. SUSY models sometimes predict a long-lived particle that can decay into LSP. Moreover, the SUSY should be extended to gravity sector. The superpartner of graviton, gravitino  $\tilde{\psi}$ , interacts with all particles, with the interaction suppressed by  $1/M_{pl}$ . Here  $M_{pl} = 2.44 \times 10^{18}$  GeV is the reduced Planck mass. Another suppressed coupling of this theory is axino( $\tilde{a}$ )-gaugino- $\gamma(Z)$  coupling, the suppression factor of which is  $g_{a\gamma}$ . It should be of the order of  $10^{-10} - 10^{-12} \text{GeV}^{-1}$  in our scenario.

Both of the interactions above are five-dimensional operators and do not directly induce very long-lived particles of our interest. Therefore, we introduce two axion and axino pairs,  $(a_1, \tilde{a}_1)$  and  $(a_2, \tilde{a}_2)$ . The decay  $\tilde{a}_2 \rightarrow a_1 a_2 \tilde{a}_1$  can be mediated by a gravitino (Fig. 6). It is suppressed by  $1/M_{pl}^4$  and may be long enough to be of interest to us. The axion energy can be monochromatic if the mass difference between  $a_2$  and the gravitino is small, so that  $a_2$  has low energy and, hence, the kinematics of  $\psi_G^*$ (virtual gravitino)  $\rightarrow a_1 \tilde{a}_1$  is approximately two body. In that case, however, we also have to worry about  $\tilde{a}_2 \rightarrow 2\gamma \tilde{a}_1$  being mediated by a gaugino exchange, which is proportional to  $(g_{a_1\gamma} g_{a_2\gamma})^2$ . The suppression of the gaugino exchange decay can be achieved if  $g_{a_2\gamma}$  is suppressed. This can be achieved if  $a_2$  belongs to a Peccei-Quinn sector that does not

directly couple to a SM gauge boson. The decay rate of  $\tilde{a}_2 \rightarrow \tilde{a}_1 a_1 a_2$  can be expressed as

$$\begin{aligned} \Gamma(\tilde{a}_2 \rightarrow \tilde{a}_1 + a_1 + a_2) &\simeq \left(\frac{1}{\sqrt{2}M_{pl}}\right)^4 \left(\frac{m_{\tilde{a}_2} + m_{\tilde{G}}}{m_{\tilde{a}_2}^2 - m_{\tilde{G}}^2}\right)^2 (m_{\tilde{a}_2} - m_{\tilde{a}_1})^7 \\ &\simeq 3.4 \times 10^{-27} [\text{s}^{-1}] \left(\frac{1\text{MeV}}{m_{\tilde{G}} - m_{\tilde{a}_2}}\right)^2 \left(\frac{m_{\tilde{a}_2} - m_{\tilde{a}_1}}{260\text{GeV}}\right)^7. \end{aligned} \quad (13)$$

Thus, in the reference scenario, although tight degeneracy in mass between  $\tilde{G}$  and  $\tilde{a}_2$  is required, monochromatic axions can be successfully produced within the favored range of the lifetime.

### 3.2 Axion production from annihilation

For the second example, we assume that a neutralino  $\tilde{\chi}^0$  is the LSP and is the dark matter. Under R-parity conservation, axions are produced by the neutralino annihilation,  $\tilde{\chi}^0 \tilde{\chi}^0 \rightarrow aa$ , via saxion s-channel exchange.

The annihilation process  $\tilde{\chi}^0 \tilde{\chi}^0 \rightarrow aa$  provides the largest cross section when  $m_s^2 \simeq q^2$ , i.e.,  $m_s \simeq 2m_{\tilde{\chi}^0}$ , and hence the width part dominates over the part of momentum transfer in the saxion propagator,

$$\begin{aligned} \sigma v(\tilde{\chi}^0 \tilde{\chi}^0 \rightarrow aa) &= \left(\frac{\alpha_k C_k}{4\pi F_a}\right)^2 \left(\frac{1}{\sqrt{2}F_a}\right)^2 \frac{1}{(q^2 - m_s^2)^2 + (m_s \Gamma_s)^2} m_{\tilde{\chi}^0}^6 \\ &\simeq 3.5 \times 10^{-28} [\text{cm}^3 \text{s}^{-1}] \left(\frac{130\text{GeV}}{m_{\tilde{\chi}^0}}\right)^2 \left(\frac{\alpha_k C_k}{10^{-2}}\right)^2, \end{aligned} \quad (14)$$

where  $F_a$  is the axion decay constant and  $\alpha_k = g_k^2/4\pi$  [ $g_k$  is the coupling constant for  $U(1)_Y$  or the  $SU(2)_L$  gauge group]. The constant  $C_k$  is the model-dependent parameter with  $\mathcal{O}(1)$  or smaller. The interaction of neutralinos and the saxion may be modified after SUSY breaking. The constant  $C_k$  also includes this uncertainty. Here we assume that the dominant decay channel of the saxion is  $s \rightarrow aa$ ; then, the decay width is  $\Gamma_s \simeq m_s^3/2F_a^2 \simeq 4m_{\tilde{\chi}^0}^3/F_a^2$ .

As shown in Fig. 4, the cross section for the axion production is required to be larger than  $10^{-27} \text{cm}^3 \text{s}^{-1}$ . For reproducing the 130 GeV  $\gamma$  rays, therefore, this type of SUSY model needs a boost factor of  $\mathcal{O}(1)$  in addition to the relation  $m_s \simeq 2m_{\tilde{\chi}^0}$ .

We currently need more precise studies of decay or annihilation processes, which should include information of dark matter profiles of the Galaxy. Other possible decay or annihilation processes of axion productions should be also studied extensively. We will discuss these issues in detail in a separate publication [85].

## 4 Summary and discussion

An excess of  $\gamma$ -ray lines in the energy range 120-140 GeV was found in public Fermi data [10]. We have proposed a scenario such that the excess is explained through the axion-photon conversion. We have shown that the  $\gamma$  rays produced via the axion-photon conversion can fit the observed narrow-line spectrum feature with the axion mass  $m_a \lesssim 10^{-6}$  eV, the Galactic magnetic field  $B \sim 1\text{-}10\mu\text{G}$ , and the axion-photon coupling constant  $g_{a\gamma} \lesssim 8.8 \times 10^{-11} \text{GeV}^{-1}$ .

We have evaluated the axion production cross section and the decay rate of heavy neutral particles for successfully fitting the 130 GeV  $\gamma$  rays. We have shown example models in particle

physics, one of which is the decaying axino scenario, and the other is the annihilating neutralino scenario. In both scenarios, a narrow-line spectrum of axions can be produced with the required cross section and decay rate.

In this work we have focused on the monoenergetic axion productions from annihilations and decays of heavy particles. The oscillation behavior of the conversion probability, however, must be considered as important. In fact, a broader spectrum of axions can fit the observed 130 GeV  $\gamma$  rays, because the oscillation dependence of the conversion probability will make a bump structure with tuning parameters (see Fig. 3).

The scenario we propose here has attractive points. First, in our scenario, the  $\gamma$ -ray line is indirectly produced by the axion-photon conversion. In the axion production, without complicated gimmicks, productions of problematic cosmic rays (e.g., continuum  $\gamma$  rays, antiprotons, and so on) are sufficiently suppressed. Second, the scenario is testable in future experiments and observations. Expected axion-photon coupling with the goal of fitting the  $\gamma$ -ray excess is just below the current bound from the CAST experiment [77]. Next-generation axion search experiments are planned to reach the favored values [86, 87]. Future  $\gamma$ -ray observations, H.E.S.S. II [88], Cherenkov Telescope Array (CTA) [89], and GAMMA-400 [90], will also observe the 130 GeV lines with much better sensitivities. We can discriminate our scenario from other models by using line shapes and the emission profile (morphology) of the spatial distribution [91, 92]. Third, our scenario would provide a probe not only into the nature of dark matter, but also into models behind the axion. In such models, axion properties are occasionally described by high-scale parameters, which are beyond the energy scale of collider experiments [93, 94]. Combining observations of  $\gamma$  rays with experimental results of the axion search will thereby shed light on the energy scale, interactions with axions and the dark matter, and so on.

Several points have to be carefully researched to test the scenario in future experiments/observations, and for the scenario to be a more sensitive probe to the nature of dark matter. First, dark matter distributions need detailed treatments. Indeed, the evaluation of  $\gamma$ -ray flux needs the spatial integral over the line of sight with dark matter profiles. However, there are still large uncertainties in both the distance from the Galactic center to the Earth and spatial distributions of the dark matter profiles. One important thing we know for certain is that dark matter density steeply damps outside of Galactic center region. Thus, as a practicable approximation, this work supposes a uniformly distributing profile localizing near the Galactic center. With improved understanding of the profiles, reevaluation of the flux should be carried out. Second, we comment on the reconversion processes  $a \rightarrow \gamma \rightarrow a$ . Large conversion probabilities will modify the observed  $\gamma$ -ray flux  $J_\gamma$  via the axion-photon conversion,  $J_\gamma \simeq (P_{a\gamma} - P_{a\gamma}^2 + \dots) \cdot J_a$ , where  $J_a$  is axion flux, and the axion production cross section or decay rate is expected to be larger than that without the reconversion processes by, at most, a factor of a few. So far, however, such modifications could not have been distinguished by any observations of  $\mathcal{O}(100\text{GeV})$   $\gamma$ -ray [11, 22]. With the current accuracy of observations, the modification does not change our conclusion that high-energy  $\gamma$ -line excess from the Galactic center can be interpreted by the axion-photon conversion without conflicting cosmic ray observations. However, in future, improvement of the observations will require precise calculation, taking into account the reconversion to confirm the scenario and determine axion parameters. Third, we mention the inverse conversion processes,  $\gamma \rightarrow a$ . Since the conversion probability in some benchmark points is large (Table 1), the  $\gamma$ -ray flux from distant sources may be attenuated by the reconversion. The attenuation can provide the observed large degree of

transparency of the universe to  $\gamma$  rays [95]. Future  $\gamma$ -ray observations will confirm our scenario by observing the predicted  $\gamma$ -ray flux from various sources, and by checking the dependence of the energy and traveling distance on the conversion probability. We will discuss these issues in detail in a separate publication [85].

## Acknowledgments

K.K. thanks K. Nakayama and O. Seto for useful discussions. This work is supported by the Grant-in-Aid for Scientific research from the Ministry of Education, Science, Sports, and Culture, Japan, Nos. 23740208, 25003345 (M.Y.), 21111006, 23540327 26105520 (K.K.), 22244030, 26247042 (K.I. and K.K.), 24103006, 24000004 (K.I.), and 23104006 (M.M.N.), and supported by the Center for the Promotion of Integrated Science (CPIS) of Sokendai (1HB5804100) (K.I. and K.K.).

## References

- [1] D. Clowe, M. Bradac, A. H. Gonzalez, M. Markevitch, S. W. Randall, C. Jones and D. Zaritsky, *Astrophys. J.* **648** (2006) L109 [astro-ph/0608407].
- [2] G. Hinshaw, D. Larson, E. Komatsu, D. N. Spergel, C. L. Bennett, J. Dunkley, M. R.olta and M. Halpern *et al.*, arXiv:1212.5226 [astro-ph.CO].
- [3] J. F. Navarro, C. S. Frenk and S. D. M. White, *Astrophys. J.* **462** (1996) 563 [astro-ph/9508025].
- [4] V. Springel, J. Wang, M. Vogelsberger, A. Ludlow, A. Jenkins, A. Helmi, J. F. Navarro and C. S. Frenk *et al.*, *Mon. Not. Roy. Astron. Soc.* **391** (2008) 1685 [arXiv:0809.0898 [astro-ph]].
- [5] M. Boylan-Kolchin, V. Springel, S. D. M. White, A. Jenkins and G. Lemson, *Mon. Not. Roy. Astron. Soc.* **398** (2009) 1150 [arXiv:0903.3041 [astro-ph.CO]].
- [6] Q. Guo, S. White, M. Boylan-Kolchin, G. De Lucia, G. Kauffmann, G. Lemson, C. Li and V. Springel *et al.*, *Mon. Not. Roy. Astron. Soc.* **413** (2011) 101 [arXiv:1006.0106 [astro-ph.CO]].
- [7] B. W. Lee and S. Weinberg, *Phys. Rev. Lett.* **39** (1977) 165.
- [8] E. W. Kolb and M. S. Turner, *The Early Universe* (Addison-Wesley, Redwood City, 1990).
- [9] E. A. Baltz, B. Berenji, G. Bertone, L. Bergstrom, E. Bloom, T. Bringmann, J. Chiang and J. Cohen-Tanugi *et al.*, *JCAP* **0807** (2008) 013 [arXiv:0806.2911 [astro-ph]].
- [10] T. Bringmann, X. Huang, A. Ibarra, S. Vogl and C. Weniger, *JCAP* **1207** (2012) 054 [arXiv:1203.1312 [hep-ph]].
- [11] W. B. Atwood *et al.* [LAT Collaboration], *Astrophys. J.* **697** (2009) 1071 [arXiv:0902.1089 [astro-ph.IM]].
- [12] A. Boyarsky, D. Malyshev and O. Ruchayskiy, *Phys. Dark Univ.* **2** (2013) 90 [arXiv:1205.4700 [astro-ph.HE]].
- [13] Y. Li and Q. Yuan, *Phys. Lett. B* **715**, 35 (2012) [arXiv:1206.2241 [astro-ph.HE]].
- [14] C. Weniger, *JCAP* **1208** (2012) 007 [arXiv:1204.2797 [hep-ph]].

- [15] E. Tempel, A. Hektor and M. Raidal, JCAP **1209** (2012) 032 [arXiv:1205.1045 [hep-ph]].
- [16] M. Su and D. P. Finkbeiner, arXiv:1206.1616 [astro-ph.HE].
- [17] D. P. Finkbeiner, M. Su and C. Weniger, JCAP **1301**, 029 (2013) [arXiv:1209.4562 [astro-ph.HE]].
- [18] D. Whiteson, JCAP **1211**, 008 (2012) [arXiv:1208.3677 [astro-ph.HE]].
- [19] A. Hektor, M. Raidal and E. Tempel, Eur. Phys. J. C **73** (2013) 2578 [arXiv:1209.4548 [astro-ph.HE]].
- [20] D. Whiteson, Phys. Rev. D **88** (2013) 023530 [arXiv:1302.0427 [astro-ph.HE]].
- [21] C. Weniger, AIP Conf. Proc. **1505**, 470 (2012) [arXiv:1210.3013 [astro-ph.HE]].
- [22] [Fermi-LAT Collaboration], arXiv:1305.5597 [astro-ph.HE].
- [23] F. Aharonian, D. Khangulyan and D. Malyshev, Astron. Astrophys. **547** (2012) A114 arXiv:1207.0458 [astro-ph.HE].
- [24] S. Profumo and T. Linden, JCAP **1207**, 011 (2012); [arXiv:1204.6047 [astro-ph.HE]].
- [25] E. Dudas, Y. Mambrini, S. Pokorski and A. Romagnoni, JHEP **1210** (2012) 123; [arXiv:1205.1520 [hep-ph]].
- [26] J. M. Cline, Phys. Rev. D **86** (2012) 015016; [arXiv:1205.2688 [hep-ph]].
- [27] K. -Y. Choi and O. Seto, Phys. Rev. D **86**, 043515 (2012) [Erratum-ibid. D **86**, 089904 (2012)]; [arXiv:1205.3276 [hep-ph]].
- [28] B. Kyae and J. -C. Park, Phys. Lett. B **718**, 1425 (2013); [arXiv:1205.4151 [hep-ph]].
- [29] H. M. Lee, M. Park and W. -I. Park, Phys. Rev. D **86** (2012) 103502; [arXiv:1205.4675 [hep-ph]].
- [30] B. S. Acharya, G. Kane, P. Kumar, R. Lu and B. Zheng, arXiv:1205.5789 [hep-ph];
- [31] M. R. Buckley and D. Hooper, Phys. Rev. D **86**, 043524 (2012); [arXiv:1205.6811 [hep-ph]].
- [32] X. Chu, T. Hambye, T. Scarna and M. H. G. Tytgat, Phys. Rev. D **86**, 083521 (2012); [arXiv:1206.2279 [hep-ph]].
- [33] D. Das, U. Ellwanger and P. Mitropoulos, JCAP **1208**, 003 (2012); [arXiv:1206.2639 [hep-ph]].
- [34] Z. Kang, T. Li, J. Li and Y. Liu, arXiv:1206.2863 [hep-ph].
- [35] L. Feng, Q. Yuan, X. Li and Y. -Z. Fan, Phys. Lett. B **720** (2013) 1 [arXiv:1206.4758 [astro-ph.HE]].
- [36] R. -Z. Yang, Q. Yuan, L. Feng, Y. -Z. Fan and J. Chang, Phys. Lett. B **715**, 285 (2012); [arXiv:1207.1621 [astro-ph.CO]].
- [37] J. -C. Park and S. C. Park, Phys. Lett. B **718** (2013) 1401; [arXiv:1207.4981 [hep-ph]].
- [38] X. -Y. Huang, Q. Yuan, P. -F. Yin, X. -J. Bi and X. -L. Chen, JCAP **1211**, 048 (2012); [arXiv:1208.0267 [astro-ph.HE]].
- [39] A. Hektor, M. Raidal and E. Tempel, arXiv:1208.1996 [astro-ph.HE];
- [40] J. M. Cline, G. D. Moore and A. R. Frey, Phys. Rev. D **86** (2012) 115013; [arXiv:1208.2685 [hep-ph]].

- [41] Y. Bai and J. Shelton, JHEP **1212** (2012) 056; [arXiv:1208.4100 [hep-ph]].
- [42] R. Laha, K. C. Y. Ng, B. Dasgupta and S. Horiuchi, Phys. Rev. D **87**, 043516 (2013); [arXiv:1208.5488 [astro-ph.CO]].
- [43] L. Bergstrom, Phys. Rev. D **86**, 103514 (2012); [arXiv:1208.6082 [hep-ph]].
- [44] L. Wang and X. -F. Han, Phys. Rev. D **87**, 015015 (2013); [arXiv:1209.0376 [hep-ph]].
- [45] S. Baek, P. Ko and E. Senaha, JHEP **1409** (2014) 153 [arXiv:1209.1685 [hep-ph]].
- [46] B. Shakya, Phys. Dark Univ. **2** (2013) 83 [arXiv:1209.2427 [hep-ph]].
- [47] Y. Farzan and A. R. Akbarieh, Phys. Lett. B **724** (2013) 84 [arXiv:1211.4685 [hep-ph]].
- [48] G. Chalons, M. J. Dolan and C. McCabe, JCAP **1302** (2013) 016 [arXiv:1211.5154 [hep-ph]].
- [49] M. Asano, T. Bringmann, G. Sigl and M. Vollmann, Phys. Rev. D **87** (2013) 103509 [arXiv:1211.6739 [hep-ph]].
- [50] A. Rajaraman, T. M. P. Tait and A. M. Wijangco, Phys. Dark Univ. **2** (2013) 17 [arXiv:1211.7061 [hep-ph]].
- [51] D. Gorbunov and P. Tinyakov, Phys. Rev. D **87** (2013) 081302 [arXiv:1212.0488 [astro-ph.CO]].
- [52] H. M. Lee, M. Park and V. Sanz, JHEP **1303** (2013) 052 [arXiv:1212.5647 [hep-ph]].
- [53] A. Biswas, D. Majumdar, A. Sil and P. Bhattacharjee, JCAP **1312** (2013) 049 [arXiv:1301.3668 [hep-ph]].
- [54] P. -H. Gu, Phys. Dark Univ. **2** (2013) 35 [arXiv:1301.4368 [hep-ph]].
- [55] J. Chen and Y. -F. Zhou, JCAP **1304** (2013) 017 [arXiv:1301.5778 [hep-ph]].
- [56] M. Endo, K. Hamaguchi, S. P. Liew, K. Mukaida and K. Nakayama, Phys. Lett. B **721** (2013) pp. 111 [arXiv:1301.7536 [hep-ph]].
- [57] C. B. Jackson, G. Servant, G. Shaughnessy, T. M. P. Tait and M. Taoso, JCAP **1307** (2013) 021 [arXiv:1302.1802 [hep-ph]].
- [58] G. Tomar, S. Mohanty and S. Rao, arXiv:1306.3646 [hep-ph].
- [59] T. Toma, Phys. Rev. Lett. **111** (2013) 091301 [arXiv:1307.6181 [hep-ph]].
- [60] F. Giacchino, L. Lopez-Honorez and M. H. G. Tytgat, JCAP **1310** (2013) 025 [arXiv:1307.6480 [hep-ph]].
- [61] T. Cohen, M. Lisanti, T. R. Slatyer and J. G. Wacker, JHEP **1210** (2012) 134 [arXiv:1207.0800 [hep-ph]].
- [62] J. Hisano, M. Kawasaki, K. Kohri, T. Moroi, K. Nakayama and T. Sekiguchi, Phys. Rev. D **83**, 123511 (2011) [arXiv:1102.4658 [hep-ph]].
- [63] W. Buchmuller and M. Garny, JCAP **1208** (2012) 035 [arXiv:1206.7056 [hep-ph]].
- [64] N. Fornengo, L. Maccione and A. Vittino, JCAP **1404** (2014) 003 [arXiv:1312.3579 [hep-ph]].
- [65] O. Adriani, G. C. Barbarino, G. A. Bazilevskaia, R. Bellotti, M. Boezio, E. A. Bogomolov, L. Bonechi and M. Bonghi *et al.*, Phys. Rev. Lett. **102** (2009) 051101 [arXiv:0810.4994 [astro-ph]].
- [66] H. Pirmakoff, Phys. Rev. **81** (1951) 899.



- [67] P. Sikivie, Phys. Rev. Lett. **51** (1983) 1415 [Erratum-ibid. **52** (1984) 695].
- [68] D. Hooper and P. D. Serpico, Phys. Rev. Lett. **99**, 231102 (2007) [arXiv:0706.3203 [hep-ph]].
- [69] M. Roncadelli, A. De Angelis and O. Mansutti, AIP Conf. Proc. **1018** (2008) 147 [arXiv:0902.0895 [astro-ph.CO]].
- [70] A. De Angelis, O. Mansutti, M. Persic and M. Roncadelli, Mon. Not. Roy. Astron. Soc. **394** (2009) L21 [arXiv:0807.4246 [astro-ph]].
- [71] M. Fairbairn, T. Rashba and S. V. Troitsky, objects - Shining light through the Universe,” Phys. Rev. D **84** (2011) 125019 [arXiv:0901.4085 [astro-ph.HE]].
- [72] N. Bassan, A. Mirizzi and M. Roncadelli, JCAP **1005** (2010) 010 [arXiv:1001.5267 [astro-ph.HE]].
- [73] M. Meyer, D. Horns and M. Raue, Phys. Rev. D **87**, **035027** (2013) [arXiv:1302.1208 [astro-ph.HE]].
- [74] J. P. Conlon and M. C. D. Marsh, arXiv:1305.3603 [astro-ph.CO].
- [75] T. Higaki, K. Nakayama and F. Takahashi, arXiv:1306.6518 [hep-ph].
- [76] H. Tashiro, J. Silk and D. J. E. Marsh, arXiv:1308.0314 [astro-ph.CO].
- [77] S. Aune *et al.* [CAST Collaboration], Phys. Rev. Lett. **107** (2011) 261302 [arXiv:1106.3919 [hep-ex]].
- [78] G. Raffelt and L. Stodolsky, Phys. Rev. D **37** (1988) 1237.
- [79] F. Eisenhauer, R. Schoedel, R. Genzel, T. Ott, M. Tecza, R. Abuter, A. Eckart and T. Alexander, Astrophys. J. **597** (2003) L121 [astro-ph/0306220].
- [80] A. Mirizzi, G. G. Raffelt and P. D. Serpico, Phys. Rev. D **76** (2007) 023001 [arXiv:0704.3044 [astro-ph]].
- [81] R. Beck and R. Wielebinski, Planets Populations (Systems) 978 [arXiv:1302.5663 [astro-ph.GA]].
- [82] G. Steigman, B. Dasgupta and J. F. Beacom, Phys. Rev. D **86** (2012) 023506 [arXiv:1204.3622 [hep-ph]].
- [83] M. Garny, A. Ibarra and D. Tran, JCAP **1208** (2012) 025 [arXiv:1205.6783 [hep-ph]].
- [84] A. Arvanitaki, S. Dimopoulos, S. Dubovsky, P. W. Graham, R. Harnik and S. Rajendran, Phys. Rev. D **79** (2009) 105022 [arXiv:0812.2075 [hep-ph]].
- [85] M. Yamanaka *et al.* in preparation.
- [86] I. G. Irastorza, F. T. Avignone, S. Caspi, J. M. Carmona, T. Dafni, M. Davenport, A. Dardarev and G. Fanourakis *et al.*, JCAP **1106** (2011) 013 [arXiv:1103.5334 [hep-ex]].
- [87] P. W. Graham and S. Rajendran, Phys. Rev. D **84** (2011) 055013 [arXiv:1101.2691 [hep-ph]].
- [88] P. Vincent for the H.E.S.S. collaboration 29th International Cosmic Ray Conference Pune (2005) **5**, 163.
- [89] M. Actis *et al.* [CTA Consortium Collaboration], Exper. Astron. **32** (2011) 193 [arXiv:1008.3703 [astro-ph.IM]].
- [90] A. M. Galper, O. Adriani, R. L. Aptekar, I. V. Arkhangelskaja, A. I. Arkhangelskiy, M. Boezio, V. Bonvicini and K. A. Boyarchuk *et al.*, AIP Conf. Proc. **1516** (2012) 288 [arXiv:1210.1457 [astro-ph.IM]].

- [91] L. Bergstrom, G. Bertone, J. Conrad, C. Farnier and C. Weniger, JCAP **1211**, 025 (2012) [arXiv:1207.6773 [hep-ph]].
- [92] C. Weniger, M. Su, D. P. Finkbeiner, T. Bringmann and N. Mirabal, arXiv:1305.4710 [astro-ph.HE].
- [93] A. D. Linde, Phys. Lett. B **201** (1988) 437.
- [94] M. P. Hertzberg, M. Tegmark and F. Wilczek, Phys. Rev. D **78** (2008) 083507 [arXiv:0807.1726 [astro-ph]].
- [95] F. Aharonian *et al.* [H.E.S.S. Collaboration], Nature **440** (2006) 1018 [astro-ph/0508073].